Supplementary Information Text

Extended Materials and Methods

Cell culture

BPH1, LNCaP, PC3, C4-2, C4-2MDVR, 22RV1, CWRR1 and DU145 cells were maintained in RPMI 1640 medium (Gibco 11875), NCI-H660 cells were cultured in RPMI 1640 medium with 1% Insulin Transferrin Selenium, 0.02‰ Hydrocortisone and 0.02‰ Beta-estradiol. LAPC4 cells were maintained in IMDM medium (Gibco 12440). RWPE1 cells were cultured in keratinocyte serum-free medium (Gibco). All medium was supplemented with 10% fetal bovine serum (FBS) (Corning) and 1% penicillin-streptomycin (Gibco). Androgen deprived therapy (ADT) in LNCaP and LAPC4 cells was carried out by using RPMI 1640 (Gibco 11835 phenol red free) and IMDM (Gibco 21056 phenol red free), respectively, supplemented with 10% charcoal dextran stripped fetal bovine serum (CS-FBS) (Denville) and 1% penicillin-streptomycin. LNCaP95 cells were cultured in RPMI 1640 (Gibco 11835) with 10% CS-FBS. Experiments of LNCaP, PC3, C4-2 and C4-2MDVR cells under deprived glutamine or deprived glucose culture conditions were performed by using RPMI 1640 medium without glutamine (Gibco 21870) or RPMI 1640 medium without glucose (Corning 10-043-CV) supplemented with sodium pyruvate (Gibco).

3'UTR luciferase assays and site-directed mutagenesis

The 3'UTR DNA fragments of human GLS1 were generated by PCR from human genomic DNA of LNCaP. The PCR products of GLS1-3'UTR were inserted into the *Renilla* luciferase plasmid pRL-CMV reporter vector (Promega) between *XbaI* and

NotI sites. The mutagenesis of GLS1-3'UTR was performed using the QuikChange II XL site-directed mutagenesis kit (Agilent Technologies). A *firefly* luciferase plasmid pGL3 control (Promega) was used to normalize the transfection efficiency. All the primer sequences for PCR, mutagenesis and sequencing are available in *SI Appendix*, Table. S1. For luciferase assay, LNCaP cells were seeded in 12-well plates. After 48 hours incubation, cells were co-transfected with 1.2 μg constructed pRL-CMV plasmid and 0.3 μg pGL3 control plasmid for 2 hours using Xfect Transfection Reagent (Clontech). Then the medium was changed to CS-FBS medium for 10 hours before addition of ethanol vehicle or 10 nM DHT for 12 hours. After 24 hours, luciferase activities were measured using the Dual-Luciferase Reporter Assay System (Promega).

Cell proliferation assay

Cells were plated in 6-well plates. For LNCaP cells, $4*10^4$ cells were seeded in 2 ml medium while for C4-2, C4-2MDVR and PC-3 cells, $1*10^4$ cells were seeded initially. To deprive glutamine or glucose, cells were plated in complete culture medium, which was replaced with glutamine-free or glucose-free medium supplemented with 10% FBS on the following day. Fresh medium was changed every three days. At the indicated time points, cells were counted using trypan blue (Gibco). MTS assay was performed in 96-well plates with initial cell number of 1000/well. For cell proliferation of ADT treatment with deprivation of glutamine/glucose and addition of glutamine/glucose experiment, medium was set up as followings: Glutamine (+)/glucose (+): glutamine, glucose and phenol red free medium (Gibco A14430)

added with 2 mM glutamine (Gibco) and 11 mM glucose (Sigma). Glutamine (-)/glucose (+): glutamine, glucose and phenol red free medium added with 11 mM glucose. Glutamine (++)/glucose (+): glutamine, glucose and phenol red free medium added with 4 mM glutamine and 11 mM glucose. Glutamine (+)/glucose (-): glutamine, glucose and phenol red free medium added with 2 mM glutamine. Glutamine (+)/glucose (++): glutamine, glucose and phenol red free medium added with 2 mM glutamine and 22 mM glucose. 1000/well LNCaP cells were seeded in 96-well plates in regular medium changed by the corresponding medium supplemented with 10% CS-FBS after cells settled down. To observe the inhibition of CB-839 (MedChemExpress), RWPE1, LNCaP and PC3 cells with the indicated concentrations of drug were seeded 1000/well in 96-well plate and incubated for 72 hours. MTS assay (Biovision) was performed to measure cell viability at the indicated time points per manufacturer's protocol. IC_{50} values were calculated using a four parameter curve fit (Graphpad Prism).

Metabolite extraction and mass spectrometry

As described previously(1), $1*10^5$ cells were plated in 6-well plates. After cells settled down, for experiment of LNCaP and LAPC4 treated by ADT, 2 ml RPMI 1640 medium (Gibco 11835) or IMDM with either regular FBS or CS-FBS were used to replace the original culture medium after being washed by cold PBS. Corresponding medium was refreshed every five days. For experiments of glutamine deprivation in comparison of LNCaP with PC3 cells, 2 ml complete RPMI 1640 medium (Gibco 11875) and RPMI 1640 glutamine free medium (Gibco 21870) were employed. At

each time point, for intracellular metabolites measurement, plates were placed on dry ice immediately. Medium was aspirated and 80% HPLC grade methanol/water was added. For measurement of metabolites extraction from medium, medium was collected in an Eppendorf tube. 100% pre-cold methanol was added to make the final concentration of methanol at 80%. Then the plates or tubes were transferred in a -80℃ freezer for 15 minutes and cells were scraped into extraction solvent. After centrifuge for 10 minutes, supernatant was transferred into a new Eppendorf tube. A speed vacuum was used to dry the samples at room temperate. The dry pellets were sent for further LC/MS analysis. Data were normalized to cell number.

^{13}C isotope tracing assay

$1*10^5$ cells were seeded in 6-well plates in 2 ml complete medium. After overnight incubation, medium was removed, washed with PBS and replaced by fresh glutamine/glucose-deprived medium (either Gibco 32404, Gibco 21870 or Gibco 11966 for LNCaP ADT glutamine-tracing, LNCaP vs PC3 and C4-2 vs C4-2MDVR glutamine-tracing or LAPC4 glucose-tracing, respectively) containing 2 mM ^{13}C-glutamine/4.5 g/L ^{13}C-glucose isotope (Cambridge). For ADT experiment, LNCaP/LAPC4 cells were treated in RPMI 1640 medium (Gibco 11835) containing either FBS or CS-FBS for two weeks prior to the tracing experiment. After 24 hours incubation with isotopomer, metabolites were extracted and sent for further LC/MS analysis.

Gene silencing and overexpression

KGA and GAC knockdown was achieved by stable transduction with shRNA

lentivirus. Lentiviral plasmids expressing shRNAs purchased from Genecopoeia (shGAC: Cat#CS-HSH058798-LVRU6MP; shKGA: Cat# CS-HSH007722-LVRU6MP) were packaged into lentivirus and infected into cells. 24 hours post-infection, cells were selected with 2 μg/ml puromycin for 7 days. Puromycin-resistant cells were pooled, amplified and analysis. AR transient knock down was performed by two sets of siRNAs purchased from Dharmacon. c-Myc-specific siRNA pool was purchased from Santa Cruz (sc-29226). Crispr sgRNA plasmids were purchased from GeneCopoeia (HCP258798-CG12-3-B). Cells were transfected by sgRNAs via Lipofectamine LTX (Invitrogen) followed by geneticin selection. Protein knockdown and knockout were confirmed by western blotting. Targeted sequences are listed in *SI Appendix*, Table. S2. For GAC and KGA overexpression, ORF plasmids were purchased from Genecopoeia (EX-T0320-Lv122 and EX-H0487-Lv105) and packaged into lentivirus for cell infection. c-Myc cDNA plasmid was a gift kindly given by Dr. Jung Wook Park(2). Overexpressed GAC, KGA and c-Myc proteins were confirmed by western blot.

RNA extraction and quantitative real-time PCR

Total RNA was extracted using RNeasy mini kits (Qiagen, Valencia, CA). The PrimeScript RT Master Mix (Takara) was used for cDNA synthesis. Quantitative real-time PCR (qRT-PCR) was performed on ABI 7500 (Applied Biosystems, Foster City, CA) using SYBR Green PCR Master Mix (Quanta Biosciences). Actin expression assay was used as an internal control. All qPCRs were performed in triplicate. The primers used are listed in *SI Appendix*, Table. S2.

Chromatin immunoprecipitation assays

Chromatin immunoprecipitation (ChIP) assays were performed as described previously(3). LNCaP cells were cultured in 5% CS-FBS medium for 3 days and then treated with either 10 nM dihydrotestosterone (DHT) or ethanol vehicle for 4 hours. Chromatin was crosslinked for 10 minutes at room temperature with 1% formaldehyde added to cell culture medium. Cell lysates were sonicated for 3 cycles, 10 seconds on, 30 seconds off using a Bioruptor sonicator (Thomas Scientific). Protein G-conjugated agarose beads were used to immunoprecipitate chromatin complexes and all subsequent steps were performed per manufacturer's protocol (Millipore). After de-crosslinking, phenol extraction and ethanol precipitation, quantitative PCR was employed on genomic DNA targets by SYBR Green PCR Master Mix (Quanta Biosciences). Primers and antibodies used are listed in *SI Appendix*, Table. S2 and S3 respectively.

Immunoblotting

Total protein lysate was collected by lysing adherent cells/tumor tissues with RIPA buffer (Sigma) supplemented with phosphatase and protease inhibitor cocktail (Thermo Fisher). Lysates were cleared by centrifugation and protein concentration in supernatant was determined by the Bradford assay kit (Bio-rad). Equal amounts of total protein were used for immunoblotting. After electrophoresis, the proteins were transferred to polyvinylidene difuoride transfer membrane (PVDF) followed by blocked in 5% non-fat milk and incubated with indicated antibodies. After washing with TBST (TBS with 0.1% Tween), corresponding secondary antibodies conjugated

with horseradish peroxidase-conjugated (HRP) were used to incubate the membranes. Samples were developed by Chemiluminescent Substrate (Thermo Fisher) and exposed by Odyssey Imaging Systems (LI-COR). The commercial antibodies used can be found in *SI Appendix*, Table. S3.

Tissue Microarrays

Several tissue microarrays were constructed and have been reported previously(4, 5). All human tissues were provided to investigators in a de-identified manner to protect patient confidentiality. Treatment-naïve samples were obtained from prostatectomy specimens including prostate cancer and the adjacent benign prostate tissue. Three cores were from benign and cancer areas of each specimen. Castration-resistant prostate cancer (CRPC) tissue microarray was built from patients who treated with hormonal therapy instead of surgery at the very beginning of prostatic adenocarcinoma diagnosis and underwent transurethral resection of prostate due to the recurred tumor which cause urinary obstruction. Tissues were histologically diagnosed as adenocarcinoma and constructed into a tissue microarray of CRPC. A small cell neuroendocrine carcinoma tissue microarray was constructed from primary small cell neuroendocrine carcinoma cases.

Immunohistochemistry

Endogenous peroxidase activity was blocked with 3% hydrogen peroxide in methanol. Heat-induced antigen retrieval (HIER) was carried out for all sections in 0.01 M citrate buffer, pH 6.0, using a steamer at 95℃. Primary antibodies were diluted with PBS containing 1% BSA and applied to the whole sections. Incubation was for 45

minutes at room temperature followed by incubation with a Dako EnVision+System-HRP Labelled Polymer for 30 minutes at room temperature. Diaminobenzidine was then applied for 10 minutes. The sections were counterstained with hematoxylin, dehydrated, coverslipped and visualized. All the primary antibodies and concentration are listed in *SI Appendix*, Table. S3. Quick-score system was performed in all the immunohistochemistry staining tissues as reported(5). The intensity of staining is multiplied by the percentage of staining to derive a composite score (a range from 0 to 300).

Colony formation assay

As described previously(6), 10^4 cells were seeded at 6 cm dishes and grown for up to 14 days with either vehicle or CB-839 treatment. Cell culture medium was refreshed every 3 days and colonies were fixed with cold methanol and then stained with 1% crystal violet. The number of colonies was counted and representative pictures were imaged with a VersaDoc Imaging System (BioRad).

Three-dimension matrigel invasion assay

As described previously(7), 1000 cells/well were seeded in the 96-well round-bottomed plates and incubated at 37℃, 5% CO2, 95% humidity to facilitate spheroid formation. After four days incubation, equal amount of matrigel was added and incubated till matrigel was solidified. Starting from time zero, and at 24-hour intervals up to 7 days, images were captured and invasive cell number and invasion distance were quantified.

Animal experiments

10^7 cells were injected subcutaneously in intact male NSG mice (Jackson Laboratories). When tumors reached ~200 mm^3, for experimental groups, mice were surgically castrated. For control groups, mice were performed with a tiny incision and suture procedure at perineum. Tumor growth was followed by caliper measurement twice a week and volumes of individual tumors were normalized to those on day 0 (day of castration). After castrated for 50 days, mice were euthanized and tumors were harvested. For long-term castration experiment, animals were euthanized after tumor recurred significantly or tumor volumes exceeded 1000 mm^3. For drug experiments, LNCaP and PC3 cells were injected subcutaneously in the mice with subsequent either vehicle or CB-839 200 mg/kg oral administration(8). Harvested tumors were embedded into paraffin followed by hematoxylin and eosin staining and immunohistochemistry staining.

Bioinformatics analysis of gene expression

Gene Set Enrichment Analysis (GSEA) was performed using GSEA v4.0.2 software (http://www.broadinstitute.org/gsea/index,jsp) with 1000 gene-set permutations using the gene-ranking metric T-test with Hallmark and GO MSigDb collections as specified in the figures. Heat-map representation of metabolite level was generated using Morpheus (Broad Institute). Datasets for determining c-Myc and N-Myc expression were retrieved from cBioPortal as well as Beltran et al, 2016. TCGA dataset was used for determining KGA and GAC variant expression and patient clinical outcomes.

Minigene assay

The gBlock, which contains exon 14-19 and their flanking intron regions of *GLS1* gene, was synthesized by Integrated DNA Technologies (IDT) and used as the template for PCR amplification. The DNA fragment product was cloned into the plasmid vector pRL-TK (Promega) between NheI and XbaI sites. DNA sequencing confirmed the integrity of the final construct, which was subsequently transfected into desired cells. KGA and GAC specific primers were used to determine the transcript levels by qPCR.

Immunocytochemical staining assay

20 million cells were harvested by washing with PBS and spun down to collect cell pellets. Using 10% formaldehyde to fix cells for 24 hours. Fixed cell pellets were further spun down to remove 10% formaldehyde and washed with PBS, followed by embedded into paraffin blocks. Antibodies were used to stain slides following immunohistochemistry procedures.

Statistical analysis

Statistically significant differences between two groups were assessed using a two-tailed paired or unpaired *t*-test. Comparisons between more than two groups were carried out by an ANOVA with Tukey's multiple-comparisons test. The Pearson correlation was used to analyze the correlation between KGA and GAC staining scores. Differences were considered statistically significant at a p value <0.05. Principal component analysis and pathway impact analysis were performed by MetaboAnalyst online software (http://www.metaboanalyst.ca/). All statistical analyses were performed using GraphPad Prism software and Microsoft Excel and R.

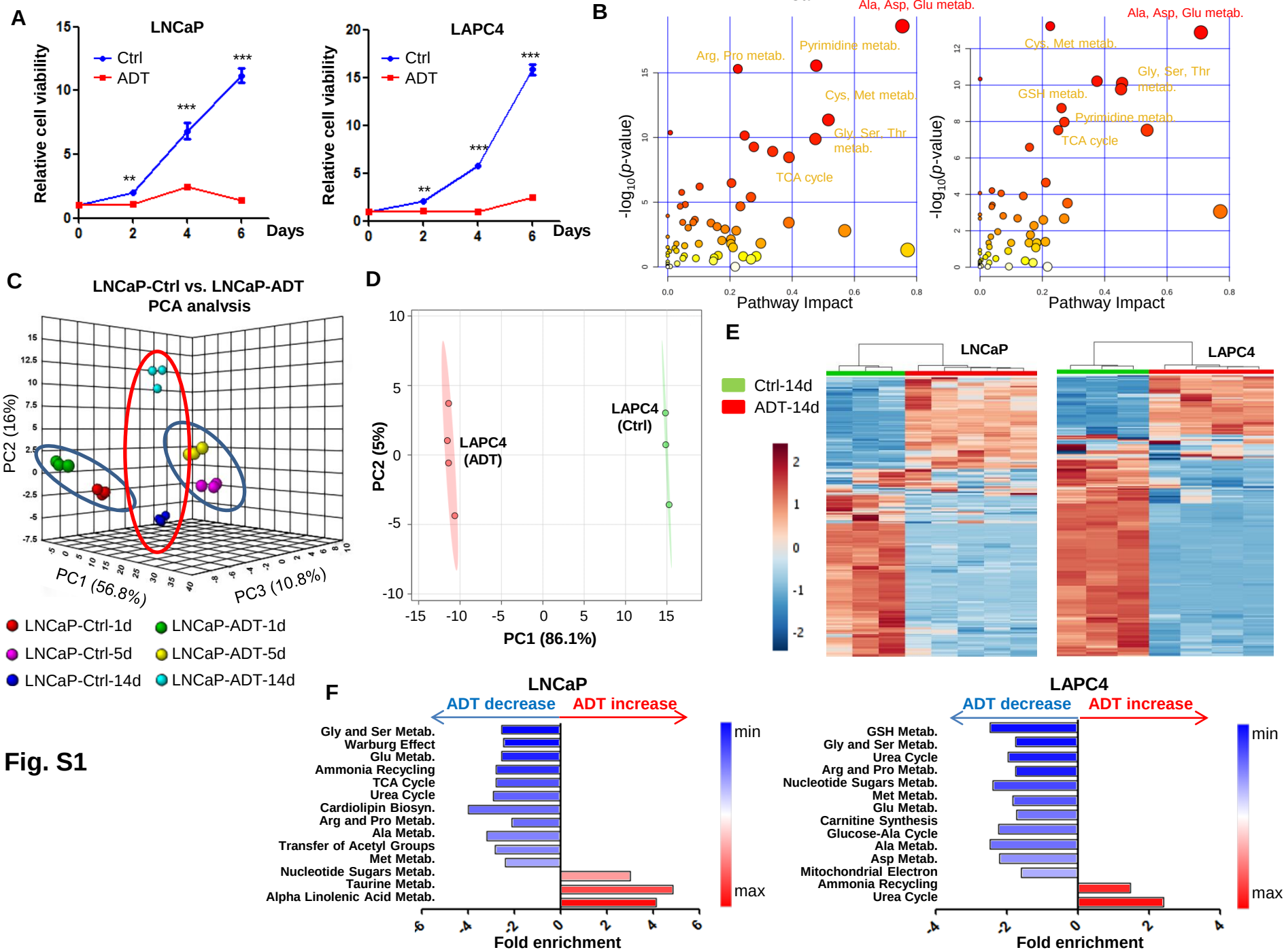
A
LNCaP
LAPC4
Ctrl
ADT
Relative cell viability
Days
B
LNCaP
LAPC4
Ala, Asp, Glu metab.
Arg, Pro metab.
Pyrimidine metab.
Cys, Met metab.
Gly, Ser, Thr metab.
TCA cycle
GSH metab.
-log10(p-value)
Pathway Impact
C
LNCaP-Ctrl vs. LNCaP-ADT
PCA analysis
PC1 (56.8%)
PC2 (16%)
PC3 (10.8%)
LNCaP-Ctrl-1d
LNCaP-ADT-1d
LNCaP-Ctrl-5d
LNCaP-ADT-5d
LNCaP-Ctrl-14d
LNCaP-ADT-14d
D
LAPC4 (ADT)
LAPC4 (Ctrl)
PC1 (86.1%)
PC2 (5%)
E
LNCaP
LAPC4
Ctrl-14d
ADT-14d
F
LNCaP
ADT decrease
ADT increase
Gly and Ser Metab.
Warburg Effect
Glu Metab.
Ammonia Recycling
TCA Cycle
Urea Cycle
Cardiolipin Biosyn.
Arg and Pro Metab.
Ala Metab.
Transfer of Acetyl Groups
Met Metab.
Nucleotide Sugars Metab.
Taurine Metab.
Alpha Linolenic Acid Metab.
Fold enrichment
min
max
LAPC4
ADT decrease
ADT increase
GSH Metab.
Gly and Ser Metab.
Urea Cycle
Arg and Pro Metab.
Nucleotide Sugars Metab.
Met Metab.
Glu Metab.
Carnitine Synthesis
Glucose-Ala Cycle
Ala Metab.
Asp Metab.
Mitochondrial Electron
Ammonia Recycling
Urea Cycle
Fold enrichment
min
max

Fig. S1

Fig. S1. Androgen deprivation therapy metabolically inhibits tumor growth. (A) Cell viability of LNCaP and LAPC4 cells treated with and without ADT (n = 3 replicates for two independent experiments). **(B)** Pathway impact analysis showing the significantly affected metabolic pathways by ADT in LNCaP and LAPC4 cells. **(C)** Principal component analysis of global metabolite changes upon androgen deprivation for LNCaP cells at day 1, day 5 and day14. **(D)** Principal component analysis of global metabolite changes upon androgen deprivation for LAPC4 cells at day 14. **(E)** Heat map analysis showing the alteration of global metabolite upon androgen withdrawal for LNCaP and LAPC4 cell at day 14. **(F)** Pathway enrichment analysis showing increased and decreased metabolic pathways after androgen withdrawal.

Fig. S2

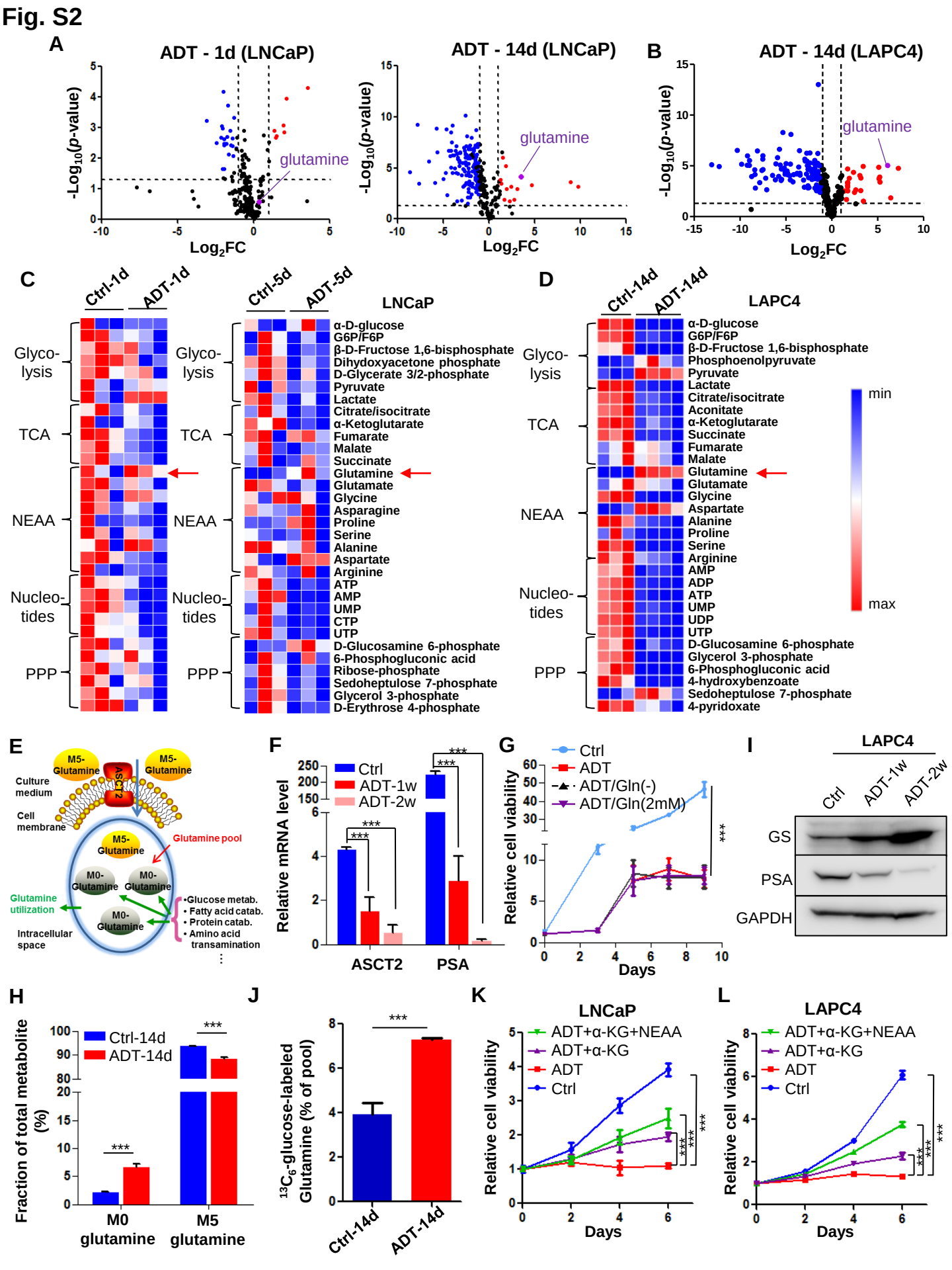
A
ADT - 1d (LNCaP)
ADT - 14d (LNCaP)
B
ADT - 14d (LAPC4)
-Log10(p-value)
Log2FC
glutamine
C
Ctrl-1d
ADT-1d
Ctrl-5d
ADT-5d
LNCaP
D
Ctrl-14d
ADT-14d
LAPC4
Glyco-lysis
TCA
NEAA
Nucleo-tides
PPP
α-D-glucose
G6P/F6P
β-D-Fructose 1,6-bisphosphate
Dihydoxyacetone phosphate
D-Glycerate 3/2-phosphate
Phosphoenolpyruvate
Pyruvate
Lactate
Citrate/isocitrate
Aconitate
α-Ketoglutarate
Fumarate
Malate
Succinate
Glutamine
Glutamate
Glycine
Asparagine
Aspartate
Proline
Alanine
Serine
Arginine
AMP
ADP
ATP
UMP
CTP
UDP
UTP
D-Glucosamine 6-phosphate
6-Phosphogluconic acid
Ribose-phosphate
Sedoheptulose 7-phosphate
Glycerol 3-phosphate
D-Erythrose 4-phosphate
4-hydroxybenzoate
4-pyridoxate
min
max
E
M5-Glutamine
ASCT2
Culture medium
Cell membrane
Glutamine pool
M0-Glutamine
Glutamine utilization
Intracellular space
•Glucose metab.
• Fatty acid catab.
• Protein catab.
• Amino acid transamination
F
Ctrl
ADT-1w
ADT-2w
Relative mRNA level
ASCT2
PSA
G
ADT
ADT/Gln(-)
ADT/Gln(2mM)
Relative cell viability
Days
I
LAPC4
Ctrl
ADT-1w
ADT-2w
GS
PSA
GAPDH
H
Ctrl-14d
ADT-14d
Fraction of total metabolite (%)
M0 glutamine
M5 glutamine
J
13C6-glucose-labeled Glutamine (% of pool)
Ctrl-14d
ADT-14d
K
LNCaP
ADT+α-KG+NEAA
ADT+α-KG
ADT
Ctrl
Relative cell viability
Days
L
LAPC4
ADT+α-KG+NEAA
ADT+α-KG
ADT
Ctrl
Relative cell viability
Days

Fig. S2. Androgen deprivation therapy leads to intracellular glutamine accumulation. (A and B) Volcano plots showing metabolite abundance in LNCaP and LAPC4 cells upon androgen deprivation at the indicated time points. **(C and D)** Heat maps showing the change of glutamine level in LNCaP and LAPC4 cells post ADT-treatment. **(E)** Schematic overview of the input and output of the intracellular glutamine pool. **(F)** Transcript level of glutamine transporter (ASCT2) and PSA upon ADT for 1 week and 3 weeks (n = 3 replicates for two independent experiments). **(G)** Relative cell viability of LNCaP cells treated with regular control media, charcoal-stripped media (ADT), ADT with depletion of glutamine (Gln) and ADT containing extra 2mM Gln (n = 3 replicates for two independent experiments). **(H)** Mass isotopomer analysis determining the intracellular M0-glutamine (synthesized from other source) and M5-glutamine (absorbed directly from culture media) levels in LNCaP cells after ADT treatment for 14 days (n = 3 cultures per group). **(I)** Western blot determining the expression of glutamine synthetase (GS) with and without androgen deprivation in LAPC4 cells. PSA was set as a positive control. **(J)** Relative fold change of glucose-labeled glutamine fraction in LAPC4 cells treated with and without ADT (n = 3 cultures per group). **(K and L)** Relative cell viability of LNCaP and LAPC4 cells treated with ADT, ADT supplemented with α-KG (6 mM) or ADT supplemented with α-KG (6 mM) and NEAA (2 mM) (n = 3 replicates for two independent experiments). Data are depicted as mean ± s.d. *** $P < 0.001$ by two-tailed Student's *t*-test.

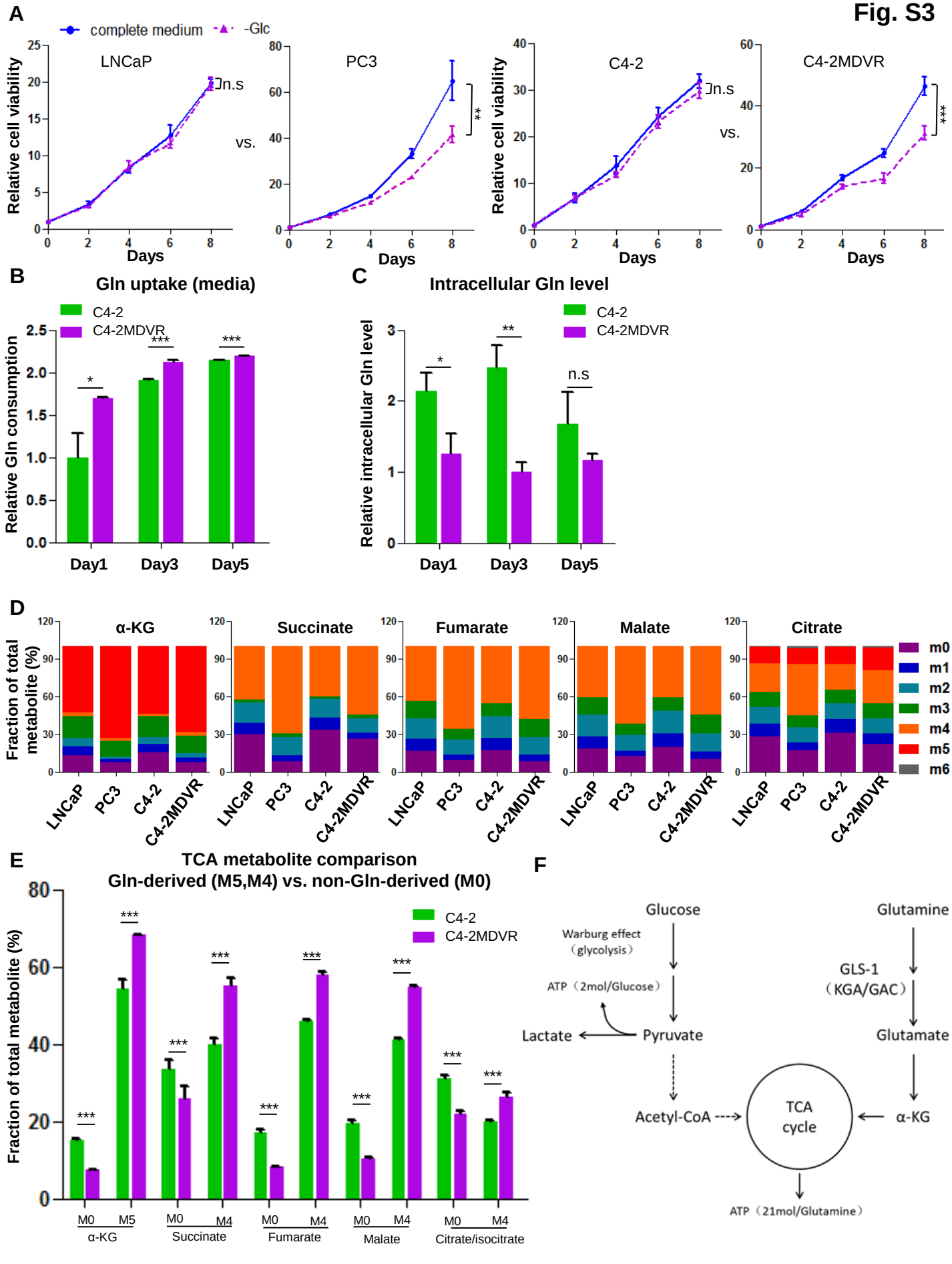
A
complete medium
-Glc
LNCaP
PC3
C4-2
C4-2MDVR
Relative cell viability
Days
n.s
vs.
**
***
B
Gln uptake (media)
C4-2
C4-2MDVR
Relative Gln consumption
Day1
Day3
Day5
C
Intracellular Gln level
Relative intracellular Gln level
n.s
D
α-KG
Succinate
Fumarate
Malate
Citrate
Fraction of total metabolite (%)
m0
m1
m2
m3
m4
m5
m6
E
TCA metabolite comparison
Gln-derived (M5,M4) vs. non-Gln-derived (M0)
Fraction of total metabolite (%)
M0
M5
M4
α-KG
Succinate
Fumarate
Malate
Citrate/isocitrate
F
Glucose
Warburg effect
(glycolysis)
ATP (2mol/Glucose)
Lactate
Pyruvate
Acetyl-CoA
TCA cycle
Glutamine
GLS-1
(KGA/GAC)
Glutamate
α-KG
ATP (21mol/Glutamine)

Fig. S3. Therapy-resistant prostate cancer cells are much more dependent on glutamine metabolism. **(A)** Relative cell viability of LNCaP, PC3, C4-2 and C4-2MDVR cells treated with or without glucose depleting in the culture medium at the indicated time points (n = 3 replicates for two independent experiments). **(B and C)** UPLC-MS analysis of glutamine uptake and intracellular glutamine levels in C4-2 and C4-2MDVR cells (n = 3 cultures per group). **(D)** [U-$^{13}C_5$] glutamine tracing experiment determining all the fractions of total intracellular glutamine pool in indicated cell lines (n = 3 cultures per group). M5-α-KG, M4-succinate, M4-Fumarate, M4-malate and M4-citrate are all from labeled glutamine. M0 represents metabolites from other source not from labeled glutamine. **(E)** Mass isotopomer analysis of TCA cycle metabolite abundance in C4-2 and C4-2MDVR cells (n = 3 cultures per group). **(F)** Model depicting glutamine anaplerosis in therapy-resistant PCa. Data are depicted as mean ± s.d. * $P < 0.05$, ** $P < 0.01$ and *** $P < 0.001$ by two-tailed Student's *t*-test. n.s., not significant.

Fig. S4

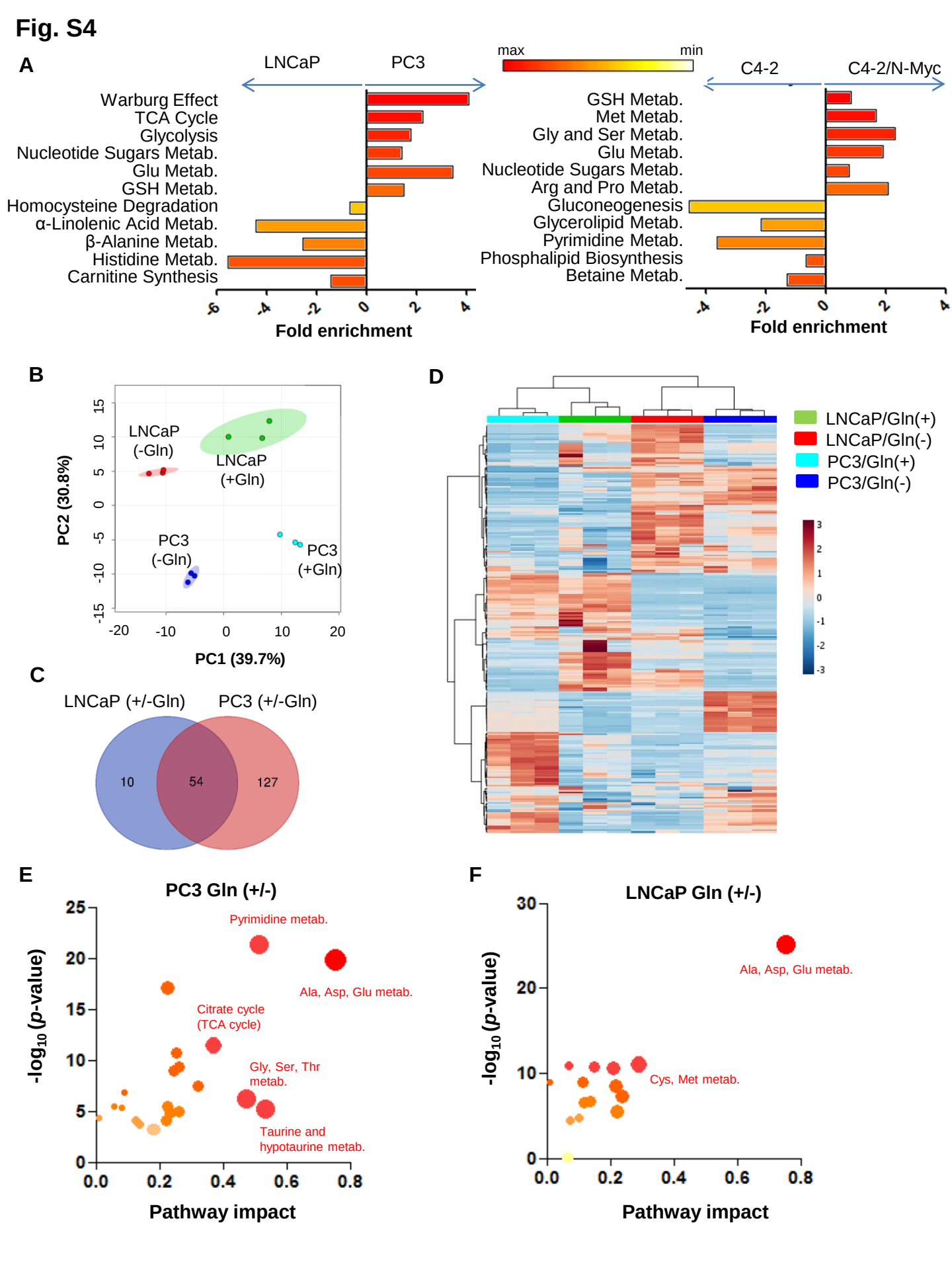
A
LNCaP
PC3
max
min
C4-2
C4-2/N-Myc
Warburg Effect
TCA Cycle
Glycolysis
Nucleotide Sugars Metab.
Glu Metab.
GSH Metab.
Homocysteine Degradation
α-Linolenic Acid Metab.
β-Alanine Metab.
Histidine Metab.
Carnitine Synthesis
GSH Metab.
Met Metab.
Gly and Ser Metab.
Glu Metab.
Nucleotide Sugars Metab.
Arg and Pro Metab.
Gluconeogenesis
Glycerolipid Metab.
Pyrimidine Metab.
Phosphalipid Biosynthesis
Betaine Metab.
Fold enrichment
Fold enrichment
B
LNCaP (-Gln)
LNCaP (+Gln)
PC3 (-Gln)
PC3 (+Gln)
PC2 (30.8%)
PC1 (39.7%)
C
LNCaP (+/-Gln)
PC3 (+/-Gln)
10
54
127
D
LNCaP/Gln(+)
LNCaP/Gln(-)
PC3/Gln(+)
PC3/Gln(-)
E
PC3 Gln (+/-)
Pyrimidine metab.
Ala, Asp, Glu metab.
Citrate cycle (TCA cycle)
Gly, Ser, Thr metab.
Taurine and hypotaurine metab.
-log10 (p-value)
Pathway impact
F
LNCaP Gln (+/-)
Ala, Asp, Glu metab.
Cys, Met metab.
-log10 (p-value)
Pathway impact

Fig. S4. Global metabolic alterations upon glutamine deprivation. (A) Pathway enrichment analysis showing the enriched metabolic pathways in the NE-like PCa cells (PC3 and C4-2/N-Myc) and their counterpart cells. **(B, C and D)** Principal component analysis, Venn diagram and heat map of global metabolite changes upon glutamine deprivation for LNCaP and PC3 cells (n = 3 replicates for each group). **(E and F)** Pathway impact analysis showing the effect of glutamine deprivation on global metabolic pathways in PC3 and LNCaP cells.

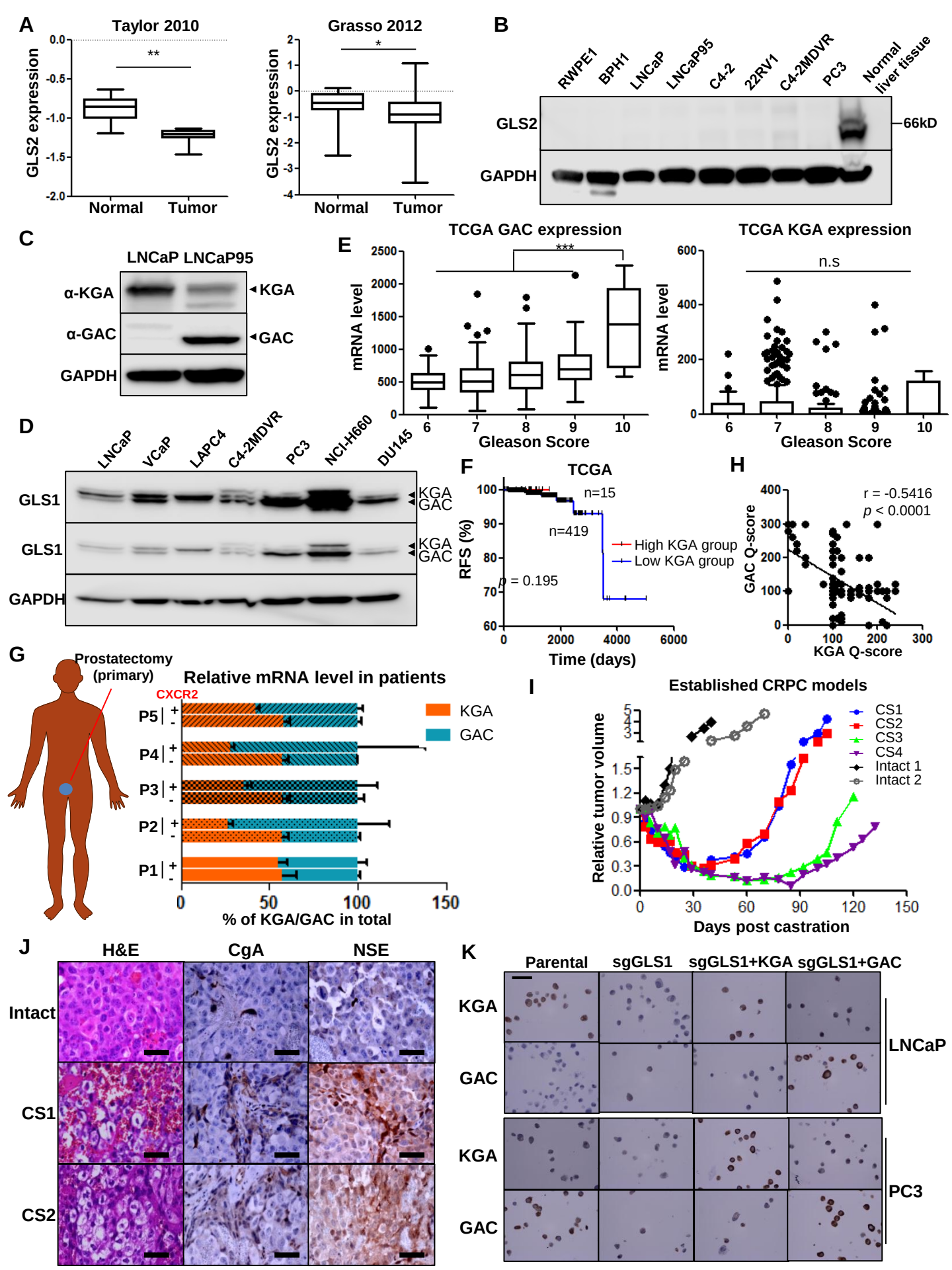
A
Taylor 2010
GLS2 expression
Normal
Tumor
Grasso 2012
B
RWPE1
BPH1
LNCaP
LNCaP95
C4-2
22RV1
C4-2MDVR
PC3
Normal liver tissue
GLS2
GAPDH
66kD
C
LNCaP LNCaP95
α-KGA
α-GAC
GAPDH
KGA
GAC
D
LNCaP
VCaP
LAPC4
C4-2MDVR
PC3
NCI-H660
DU145
GLS1
GLS1
GAPDH
KGA
GAC
E
TCGA GAC expression
TCGA KGA expression
mRNA level
Gleason Score
n.s
F
TCGA
RFS (%)
n=15
n=419
p = 0.195
High KGA group
Low KGA group
Time (days)
H
r = -0.5416
p < 0.0001
GAC Q-score
KGA Q-score
G
Prostatectomy (primary)
Relative mRNA level in patients
CXCR2
KGA
GAC
% of KGA/GAC in total
I
Established CRPC models
Relative tumor volume
Days post castration
CS1
CS2
CS3
CS4
Intact 1
Intact 2
J
H&E
CgA
NSE
Intact
CS1
CS2
K
Parental
sgGLS1
sgGLS1+KGA
sgGLS1+GAC
KGA
GAC
LNCaP
PC3

Fig. S5. GLS1 switches the isoform from KGA to GAC alongside disease progression. (A) GLS2 mRNA levels in normal prostatic tissues and PCa tissues. **(B)** Western blot determining GLS2 protein level in a panel of prostatic cell lines. Liver tissue sample is set as a positive control. **(C)** Western blot showing the differential expression of KGA and GAC in LNCaP and LNCaP95 cells detected by KGA and GAC specific antibodies. **(D)** Western blot showing GLS1 protein levels in a panel of androgen-dependent and androgen-independent PCa cell lines. Top GLS1 band was developed with longer exposure time. **(E)** mRNA levels of KGA and GAC in TCGA PCa tissues with different Gleason grades. **(F)** Recurrence-free survival (RFS) of patients stratified by KGA mRNA expression in TCGA dataset. Log rank (Mantel-Cox) test. **(G)** Transcript levels of KGA and GAC in CXCR2-positive NE-like and CXCR2-negative luminal-like cells sorted from fresh PCa tissues. **(H)** The Pearson analysis determining the correlation between KGA and GAC staining scores in adenocarcinoma, CRPC and SCNC TMA tissues. **(I)** Tumor growth curves of LNCaP xenografts showing the established CRPC animal models upon surgical castration (CS) and the corresponding intact tumors. Day 0 denotes the surgical castration time point. **(J)** Hematoxylin and eosin staining (H&E) and IHC staining for detecting NE markers CgA, NSE and SYP expression in intact tumors and CRPC tumors (CS). Scale bar, 40 μm. **(K)** Immunocytochemical staining on genetically modified prostate cancer cell lines of GLS1 knockout and specific KGA or GAC expression to confirm the specificity of the antibodies. Scale bar, 40 μm.

Fig. S6

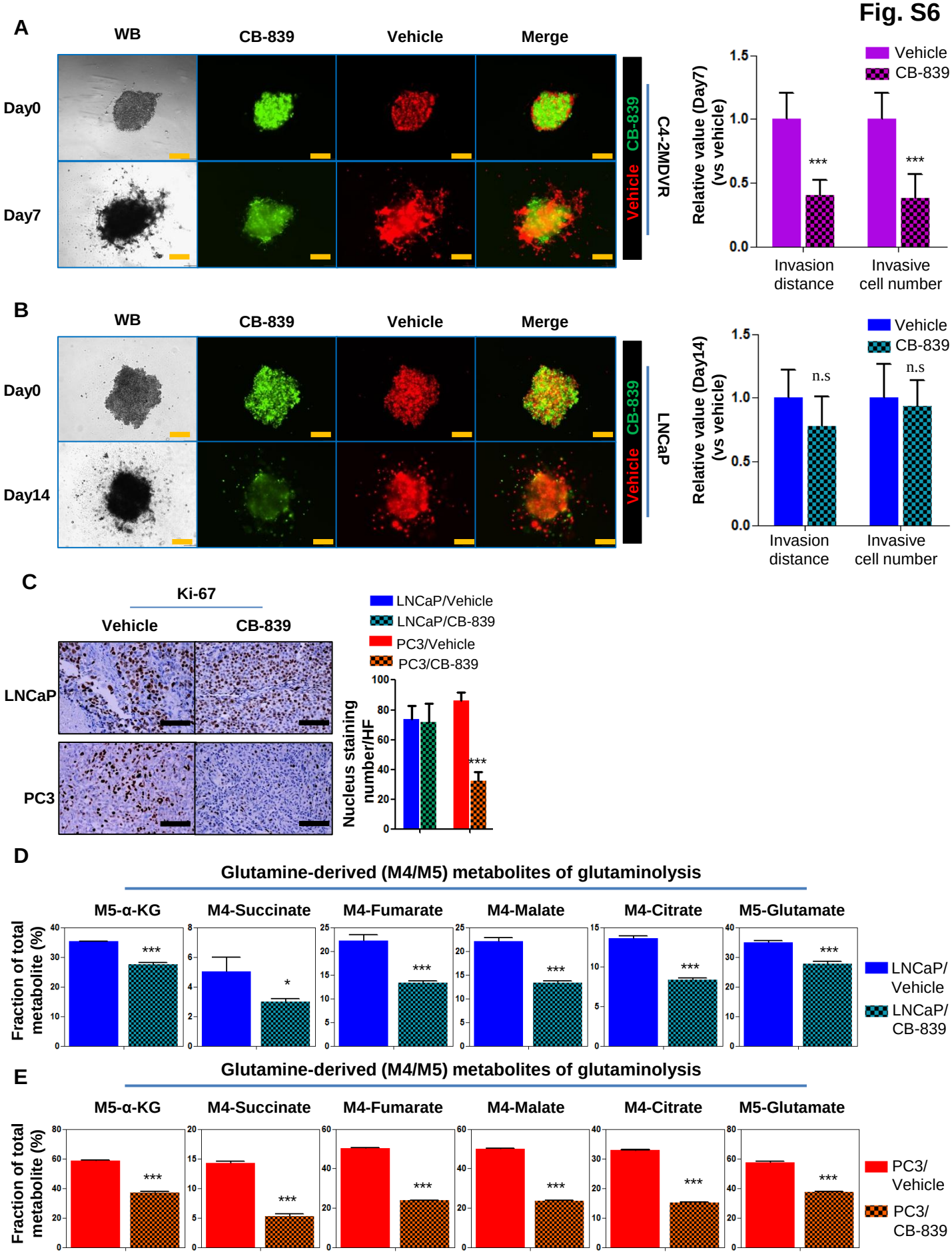
A
WB
CB-839
Vehicle
Merge
Day0
Day7
Vehicle CB-839
C4-2MDVR
Relative value (Day7) (vs vehicle)
Vehicle
CB-839
***
Invasion distance
Invasive cell number
B
Day14
LNCaP
Relative value (Day14) (vs vehicle)
n.s
C
Ki-67
LNCaP
PC3
LNCaP/Vehicle
LNCaP/CB-839
PC3/Vehicle
PC3/CB-839
Nucleus staining number/HF
D
Glutamine-derived (M4/M5) metabolites of glutaminolysis
M5-α-KG
M4-Succinate
M4-Fumarate
M4-Malate
M4-Citrate
M5-Glutamate
Fraction of total metabolite (%)
LNCaP/ Vehicle
LNCaP/ CB-839
E
PC3/ Vehicle
PC3/ CB-839

Fig. S6. GLS1 selective inhibitor CB-839 exhibits a more profound inhibitory effect on therapy-resistant prostate cancer. (A and B) Spheroid invasion assay determining the inhibitory effect of CB-839 on the migration of C4-2MDVR and LNCaP cells (n = 3 replicates for two independent experiments). Representative images (left) and quantifications of relative invading cells (right) are shown. Cells labeled RFP or GFP denote those cultured with vehicle or CB-839, respectively. Scale bar, 200 μm. **(C)** IHC staining for the LNCaP and PC3 xenograft tumors to determine the expression of proliferative markers (Ki67). Scale bar, 40 μm. **(D and E)** Mass isotopomer analysis of glutamine-derived intermediates level in LNCaP and PC3 cells after treatment with vehicle or CB-839 for 72 hours (n = 3 cultures per group). Data are depicted as mean ± s.d. * $P < 0.05$ and *** $P < 0.001$ by two-tailed Student's *t*-test. n.s., not significant.

Fig. S7

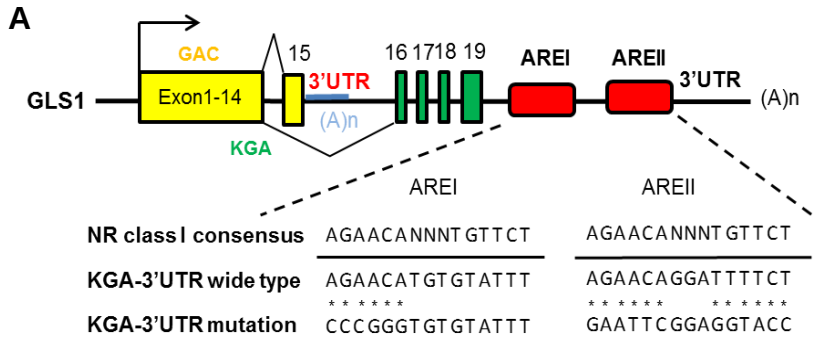
A
GAC
15
3'UTR
16 1718 19
AREI
AREII
3'UTR
GLS1
Exon1-14
(A)n
KGA
AREI
AREII
NR class I consensus
AGAACANNNTGTTCT
AGAACANNNTGTTCT
KGA-3'UTR wide type
AGAACATGTGTATTT
AGAACAGGATTTTCT
KGA-3'UTR mutation
CCCGGGTGTGTATTT
GAATTCGGAGGTACC

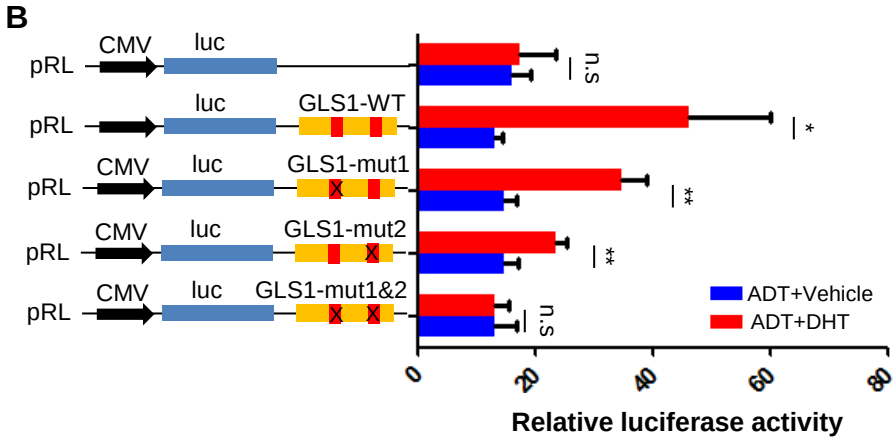
B
pRL
CMV
luc
n.s
GLS1-WT
*
GLS1-mut1
**
GLS1-mut2
**
GLS1-mut1&2
n.s
ADT+Vehicle
ADT+DHT
0
20
40
60
80
Relative luciferase activity

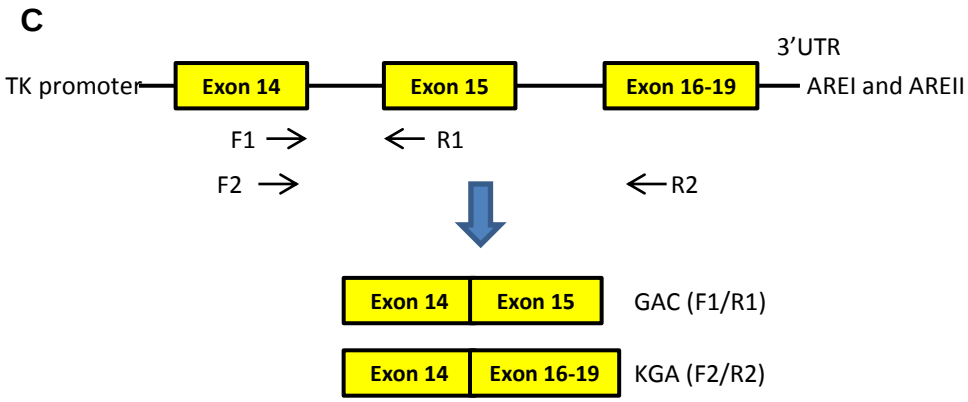
C
3'UTR
TK promoter
Exon 14
Exon 15
Exon 16-19
AREI and AREII
F1
R1
F2
R2
Exon 14
Exon 15
GAC (F1/R1)
Exon 14
Exon 16-19
KGA (F2/R2)

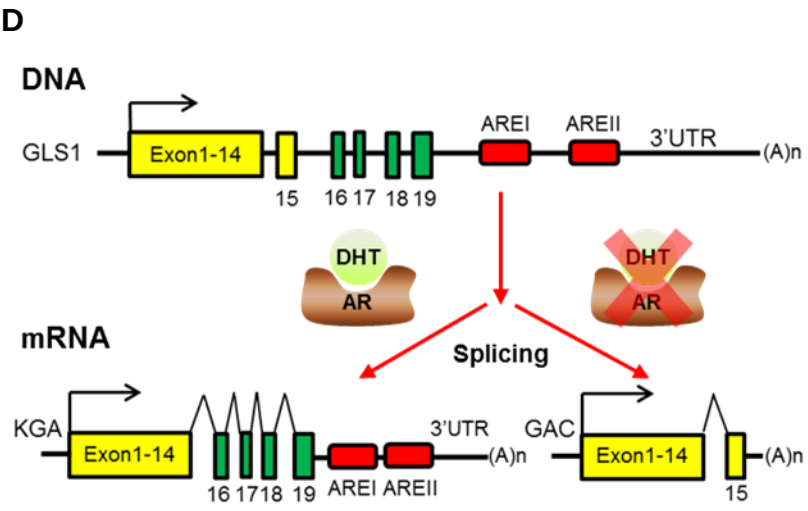
D
DNA
GLS1
Exon1-14
AREI
AREII
3'UTR
(A)n
15
16 17 18 19
DHT
AR
DHT
AR
mRNA
Splicing
KGA
Exon1-14
3'UTR
(A)n
16 1718 19
AREI AREII
GAC
Exon1-14
(A)n
15

Fig. S7. *GLS1* gene is regulated by transcription-coupled RNA splicing of AR. (A) Structure of GLS1 with two putative androgen response elements (AREI and II) identified in GLS1-3'UTR. Asterisk signs denote mutated sites. **(B)** Luciferase activity of pRL and modified constructs containing wild type (wt) GLS1-3'UTR or mutant (mut) GLS1-3'UTR (n = 3 replicates per group). Schematic of luciferase reporter constructs are shown on the left. **(C)** Diagram of the GLS1 minigene reporter. Exons, introns and PCR primers used to detect exon splicing are indicated in the diagram. Splicing between exons 14 and 15 reflects formation of GAC mRNA, which can be detected by the F1/R1 primer pair. Splicing between exons 14 and 16-19 reflects formation of KGA mRNA, which can be detected by the F2/R2 primer pair. **(D)** Working model depicting AR-mediated *GLS1* gene transcription and splicing. Data are depicted as mean ± s.d. * $P < 0.05$, ** $P < 0.01$ and *** $P < 0.001$ by two-tailed Student's *t*-test. n.s., not significant.

Fig. S8

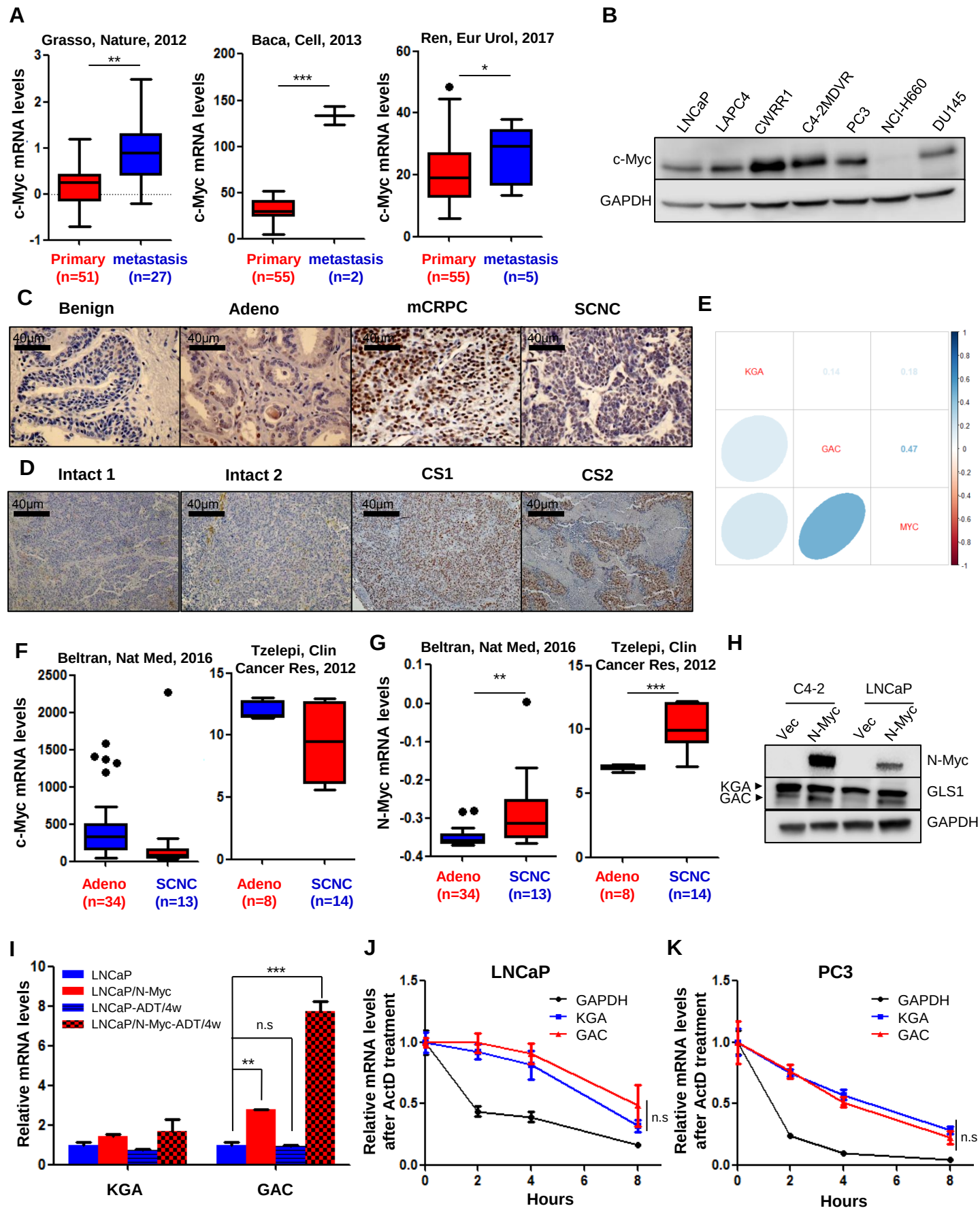
A
Grasso, Nature, 2012
Baca, Cell, 2013
Ren, Eur Urol, 2017
c-Myc mRNA levels
Primary (n=51)
metastasis (n=27)
Primary (n=55)
metastasis (n=2)
Primary (n=55)
metastasis (n=5)
B
LNCaP
LAPC4
CWRR1
C4-2MDVR
PC3
NCI-H660
DU145
c-Myc
GAPDH
C
Benign
Adeno
mCRPC
SCNC
40μm
D
Intact 1
Intact 2
CS1
CS2
E
KGA
GAC
MYC
0.14
0.18
0.47
F
Beltran, Nat Med, 2016
Tzelepi, Clin Cancer Res, 2012
c-Myc mRNA levels
Adeno (n=34)
SCNC (n=13)
Adeno (n=8)
SCNC (n=14)
G
Beltran, Nat Med, 2016
Tzelepi, Clin Cancer Res, 2012
N-Myc mRNA levels
Adeno (n=34)
SCNC (n=13)
Adeno (n=8)
SCNC (n=14)
H
C4-2
LNCaP
Vec
N-Myc
KGA
GAC
N-Myc
GLS1
GAPDH
I
LNCaP
LNCaP/N-Myc
LNCaP-ADT/4w
LNCaP/N-Myc-ADT/4w
Relative mRNA levels
n.s
KGA
GAC
J
LNCaP
GAPDH
KGA
GAC
Relative mRNA levels after ActD treatment
n.s
Hours
K
PC3
GAPDH
KGA
GAC
Relative mRNA levels after ActD treatment
n.s
Hours

Fig. S8. MYC induces GAC expression. **(A)** c-Myc mRNA level in primary and metastatic PCa tissues. **(B)** Western blot determining c-Myc protein level in a panel of PCa cell lines. **(C)** IHC staining of c-Myc expression in benign prostate, adenocarcinoma, mCRPC and SCNC tissues. Scale bar, 40 μm. **(D)** IHC staining of c-Myc expression in intact and surgical castration (CS)-induced CRPC animal tumors. Scale bar, 40 μm. **(E)** Correlation analysis between KGA, GAC and c-Myc transcript level in TCGA dataset. **(F and G)** c-Myc and N-Myc mRNA levels in adenocarcinoma and SCNC tissues. **(H)** Western blot determining KGA and GAC expression by probed with GLS1 antibody after overexpressing N-Myc in C4-2 and LNCaP cells. **(I)** Transcript level of KGA and GAC in LNCaP cells with N-Myc overexpression, ADT treatment or combination (n = 3 replicates per group). **(J and K)** KGA and GAC transcript levels in LNCaP and PC3 cells after actinomycin D (ActD) treatment at indicated time points (n = 3 replicates per group). Results were normalized to 18s rRNA, whose level was not affected by ActD treatment. GAPDH was set a positive control. Data are depicted as mean ± s.d. * $P < 0.05$, ** $P < 0.01$ and *** $P < 0.001$ by two-tailed Student's *t*-test. n.s., not significant.

Table S1. Primers used for PCR, mutagenesis and sequencing in luciferase assay study.

Name	Sequence	Comments
GLS1-3'UTR-PCR-F	ATATAAATCTAGATGGTCTCAAATCCCAAGATTTAAATCACTT	*XbaI*/*NotI* linker for GLS1-3'UTR PCR products, cloned into pRL-CMV plasmid
GLS1-3'UTR-PCR-R	TTTAATAGCGGCCGCGATACATATATTTATTATGCTGTAAAAAGCAA	
GLS1-3'UTR-AREI-mut-F	GTGGAAAATGATTATGAcccgggTGTATTTCTATCTGGTAGTGATG	Mutate sites AGAACA (AREI) to CCCGGG (*SmaI)*
GLS1-3'UTR-AREI-mut-R	CATCACTACCAGATAGAAATACAcccgggTCATAATCATTTTCCAC	
GLS1-3'UTR-AREII-mut1-F	GGGGCTTCAAAAAACGGATgaattcGGATTTTCTAGGAGTTACACATAC	Mutate sites AGAACA (AREII1) to GAATTC (*EcoRI*)
GLS1-3'UTR-AREII-mut1-R	GTATGTGTAACTCCTAGAAAATCCgaattcATCCGTTTTTTGAAGCCCC	
GLS1-3'UTR-AREII-mut1-2-F	GGGGCTTCAAAAAACGGATgaattcGGAggtaccAGGAGTTACACATAC	Mutate sites TTTTCT (AREII2) to GGTACC (*KpnI*)
GLS1-3'UTR-AREII-mut1-2-R	GTATGTGTAACTCCTggtaccTCCgaattcATCCGTTTTTTGAAGCCCC	
pRL-GLS1-3'UTR-seq-F	AGATGCACCTGATGAAATGGGA	Primers for modified reporter plasmids sequencing
pRL-GLS1-3'UTR-seq-R	AGCATTTTTTTCACTGCATTCTAGTTGT	
GLS1-3'UTR-AREI-mut-seq-F	AGATGCACCTGATGAAATGGGA	Primers for GLS1-3'UTR AREI mutation sites sequencing
GLS1-3'UTR-AREI-mut-seq-R	AGACATTTTAAACACACAACCGT	
GLS1-3'UTR-AREII-mut-seq-F	AGTAAGTCAGAAAATGCCTCCTAT	Primers for GLS1-3'UTR AREII mutation sites sequencing
GLS1-3'UTR-AREII-mut-seq-R	GCTTAATATCAGAACTCCTCACTAAC	

Table S2. PCR, qPRC primers and shRNA targeted sequences used in this study.

Gene	Sequence	Description
KGA-F	ACTGGAGATGTGTCTGCACTTCGAAG	qPCR primer
KGA-G	CCAAAGTGCAGTGCTTCATCCATGGGAGTG	qPCR primer
GAC-F	TTGGACTATGAAAGTCTCCAACAAGAAC	qPCR primer
GAC-R	CCATTCTATATACTACAGTTGTAGAGATGTCCTC	qPCR primer
GLS1-F	TGCATTCCTGTGGCATGTAT	qPCR primer
GLS1-R	TTGCCCATCTTATCCAGAGG	qPCR primer
SLC1A5-F	CATCATCCTCGAAGCAGTCA	qPCR primer
SLC1A5-R	CTCCGTACGGTCCACGTAAT	qPCR primer
PSA-F	GATGAAACAGGCTGTGCCG	qPCR primer
PSA-R	CCTCACAGCTACCCACTGCA	qPCR primer
Actin-F	AGAGCTACGAGCTGCCTGAC	qPCR primer
Actin-R	AGCACTGTGTTGGCGTACAG	qPCR primer
KGA shRNA1	GGGTAAAGTCAGTGATAAATC	shRNA targeted sequence
KGA shRNA2	GCACTTCGAAGATTTGCTTTG	shRNA targeted sequence
KGA shRNA3	GAACAGCGGGACTATGATTCT	shRNA targeted sequence
KGA shRNA4	GAATAACACTCCCATGGATGA	shRNA targeted sequence
GAC shRNA1	CTTTGGACCATTGGACTATGA	shRNA targeted sequence
GAC shRNA2	GTCAAATGAGGACATCTCTAC	shRNA targeted sequence
GAC shRNA3	GAATGGAAAGTCTGGGAGAGA	shRNA targeted sequence
GAC shRNA4	GCAGGTAGTAAGTATGCTACT	shRNA targeted sequence
GLS1-ChIP-F	TGGTCTCAAATCCCAAGATTTAAAT	ChIP-qPRC primer
GLS1-ChIP-R	GACAGGATAAAATGTATGTGTAACTCC	ChIP-qPRC primer
PSA-enh-ChIP-F	TGGGACAACTTGCAAACCTG	ChIP-qPRC primer
PSA-enh-ChIP-R	CCAGAGTAGGTCTGTTTTCAATCCA	ChIP-qPRC primer

Table S3. Antibodies used in this study

Assay	Antibody	Company	Cat#	Dilution
WB	Glutaminase	Abcam	Ab93434	1:1000
	KGA	Proteintech	20170-1-AP	1:1000
	GAC	Proteintech	19958-1-AP	1:1000
	PSA	Dako	A0562	1:200
	ASCT2	Cell Signaling	8057	1:1000
	GS	Santa Cruz	sc-74430	1:200
	AR	Millipore	ab561	1:1000
	GAPDH	Abcam	ab9484	1:5000
	GLS2	Abcam	ab113509	1:1000
	c-Myc	Abcam	ab32072	1:1000
	N-Myc	Santa Cruz	sc-53993	1:200
	β-actin	Sigma	A5441	1:3000
IHC	KGA	Proteintech	20170-1-AP	1:800
	GAC	Proteintech	19958-1-AP	1:100
	Synaptophysin	Biocare	CM371	1:100
	Chromogranin A	Thermo Fisher	PA5-32349	1:500
	NSE	Abcam	ab53025	1:200
	Ki67	Thermo Fisher	RM-9106	1:300
	c-Myc	Abcam	ab32072	1:100
ChIP	AR	Abcam	ab74272	1 μ g/ml
	IgG	Millipore	12-370	1 μ g/ml

SI References

1. Pan M*, et al.* (2016) Regional glutamine deficiency in tumours promotes dedifferentiation through inhibition of histone demethylation. *Nat Cell Biol* 18(10):1090-1101.
2. Park JW*, et al.* (2018) Reprogramming normal human epithelial tissues to a common, lethal neuroendocrine cancer lineage. *Science* 362(6410):91-95.
3. Wang QB, Carroll JS, & Brown M (2005) Spatial and temporal recruitment of androgen receptor and its coactivators involves chromosomal looping and polymerase tracking. *Mol Cell* 19(5):631-642.
4. Huang JT*, et al.* (2005) Differential expression of interleukin-8 and its receptors in the neuroendocrine and non-neuroendocrine compartments of prostate cancer. *Am J Pathol* 166(6):1807-1815.
5. Park JW, Lee JK, Witte ON, & Huang J (2017) FOXA2 is a sensitive and specific marker for small cell neuroendocrine carcinoma of the prostate. *Modern pathology : an official journal of the United States and Canadian Academy of Pathology, Inc* 30(9):1262-1272.
6. Yin Y*, et al.* (2019) N-Myc promotes therapeutic resistance development of neuroendocrine prostate cancer by differentially regulating miR-421/ATM pathway. *Molecular cancer* 18(1):11.
7. Vinci M, Box C, & Eccles SA (2015) Three-Dimensional (3D) Tumor Spheroid Invasion Assay. *Jove-J Vis Exp* (99).
8. Gross MI*, et al.* (2014) Antitumor activity of the glutaminase inhibitor CB-839 in triple-negative breast cancer. *Molecular cancer therapeutics* 13(4):890-901.